CROATICA CHEMICA ACTA CCACAA **75** (2) 447–473 (2002)

ISSN-0011-1643
CCA-2811

Original Scientific Paper

Riemann Surfaces as Descriptors for Symmetrical Negative Curvature Carbon and Boron Nitride Structures*

R. Bruce King

Department of Chemistry, University of Georgia,
Athens, Georgia 30602, USA
(E-mail: rbking@sunchem.chem.uga.edu)

Received April 27, 2001; revised August 28, 2001; accepted September 5, 2001

Leapfrog transformations starting with the genus 3 Klein and Dyck tessellations consisting of 24 heptagons and 12 octagons, respectively, can generate possible highly symmetrical structures for allotropes of carbon and the isosteric boron nitride, $(BN)_x$. The Klein tessellation, alternatively described as a platonic {3,7} tessellation, corresponds to the Riemann surface for the multi-valued function $w = \sqrt[7]{z(z-1)^2}$, which can also described by the homogeneous quartic polynomial $\xi^3\eta + \eta^3\omega + \omega^3\xi = 0$. The symmetry of this polynomial is related to the heptakisoctahedral automorphism group of the Klein tessellation of order 168. Similarly the Dyck or {3,8} tessellation can be described by a Riemann surface which corresponds to the homogeneous Fermat quartic polynomial $\xi^4 + \eta^4 + \omega^4 = 0$. The symmetry of the Fermat quartic relates to the automorphism group of the Dyck tessellation of order 96.

Key words: Riemann Surface, boron nitride, leapfrog transformation, Klein tessellation, Dyck tessellation.

INTRODUCTION

Until the 1980's diamond and graphite were the only well-characterized allotropes of elemental carbon. The structure of diamond is well known to consist of an infinite three-dimensional network of tetrahedral sp^3 carbon

* This paper is dedicated to Milan Randić in recognition of his pioneering contributions to mathematical chemistry.

atoms whereas the structure of graphite consists of an infinite planar network of hexagons of trigonal sp^2 carbon atoms. During the 1980's new allotropes of carbon were discovered exhibiting finite molecular cage structures rather than the infinite polymeric structures of diamond and graphite; such carbon allotropes have been named fullerenes. The key feature of the structures of such fullerenes is the presence of pentagons as well as hexagons of trigonal carbon atoms. The best known and most symmetrical fullerene is C_{60}, which is now well known to have a truncated icosahedral structure of I_h point group symmetry.[1] The substitution of pentagons for some of the hexagons in the graphite structure converts the zero curvature infinite flat graphite structure into a positive curvature finite polyhedral structure.

A question of interest is the favored shapes of networks of trigonal carbon atoms in which some of the hexagons of graphite are replaced by heptagons. Such networks do not correspond to positive curvature surfaces leading to finite polyhedra but instead to negative curvature surfaces[2] leading to infinite structures known as infinite periodic minimal surfaces (IPMS's).[3] Mackay and Terrones[4] in 1991 apparently first recognized the possibility of such negative curvature allotropes of carbon. In 1992 Vanderbilt and Tersoff[5] first postulated the so-called D168 structure with a unit cell of genus three containing 24 heptagons and 56 hexagons and a total of 168 carbon atoms. In 1996 the author[6] first pointed out the connection between this D168 carbon structure and a genus three surface tessellated with 24 heptagons first described by the German mathematician Felix Klein in 1879 (Ref. 7) which is conveniently called the Klein tessellation. Thus the relationship between the Klein tessellation and the D168 structure through a so-called leapfrog transformation[8–12] was found to be completely analogous to the relationship between the regular dodecahedron and the truncated icosahedron of C_{60}. The permutational symmetry of the Klein tessellation and thus the D168 structure could be described by a simple permutation group of order 168, which has been called the heptakisoctahedral group, ^7O, because of its origin from the octahedral group by adding seven-fold symmetry.[13] The heptakisoctahedral group also bears a relationship to the icosahedral group since it can be generated from a finite field of seven elements by a procedure analogous to the generation of the icosahedral (or pentakistetrahedral group)[13] from a finite field of five elements.

A similar approach can be used to describe structures of carbon or isosteric boron nitride allotropes consisting only of hexagons and octagons.[14] In this case the relevant figure is a genus three surface tessellated with 12 octagons, which was first described in 1880 by Walther von Dyck,[15] a contemporary of Felix Klein. The relevant permutation group is a group of order 96, which has a normal subgroup chain leading to the trivial group C_1

through subgroups of order 48 and 16 not related to the octahedral or tetrahedral groups.

This paper presents an alternative method for studying IPMS structures, such as those found in carbon or boron nitride allotropes or some zeolites[16] based on Riemann surfaces tessellated with polygons. The geometrical construction now known as a Riemann surface was first developed by Riemann in the 19th century for the study of multi-valued functions, of which $w = \sqrt{z}$ is a trivial example. Riemann surfaces played a major role in the 19th century in the development of the theory of elliptic functions.[17] The Klein and Dyck tessellations mentioned above can be considered as genus 3 Riemann surfaces tessellated with heptagons and octagons, respectively, related to homogeneous polynomials of degree 4. This paper develops the relevant theory of Riemann surfaces by first considering simpler examples including a genus 1 Riemann surface related to elliptic integrals and a genus 2 Riemann surface of pentagonal bipyramidal symmetry.

POLYHEDRAL POLYNOMIALS AND RIEMANN SURFACES

The usual types of convex polyhedra, including the five regular polyhedra (Figure 1), can be represented as points on the surface of a sphere. The same sphere, taken as a special unit sphere called the Riemann sphere, can also be used to represent the complex numbers $z = a + bi$. Such spheres provide a method for generating special polynomials associated with a given polyhedron. In this connection, first represent the complex numbers $z = a + bi$

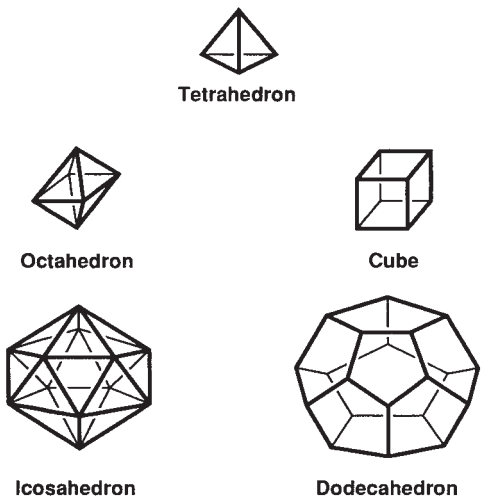

Figure 1. The five regular (platonic) polyhedra.

by points on the (x,y) plane with the x-coordinate corresponding to a and the y-coordinate corresponding to b; such a plane is called an Argand plane (Figure 2). The Argand plane can then be mapped onto the Riemann sphere (Figure 2) so that the North Pole is ∞ and the South Pole is 0; the 0–∞ axis can be called the polar axis.[18] The equation of the Riemann sphere is taken to be $p^2 + q^2 + r^2 = 1$.

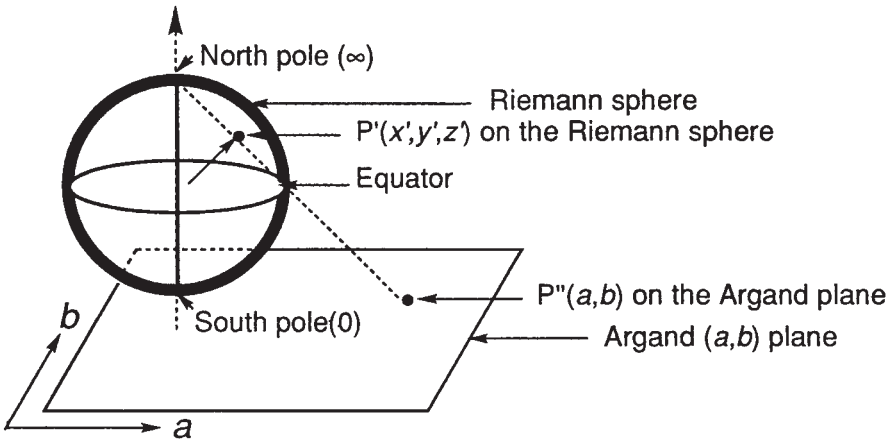

Figure 2. Projection of the Argand plane for the complex number $z = a + bi$ onto the Riemann sphere.

The polyhedral polynomials are polynomials whose roots correspond to the locations of the polyhedral vertices, the midpoints of the polyhedral edges, or the midpoints of the polyhedral faces on the surface of the Riemann sphere. Polyhedral polynomials are frequently expressed in terms of homogeneous variables so that all terms are the same combined degree in two variables, *i.e.*,

$$\sum_{i=1}^{n} a_{n-i} x^i = \sum_{i=1}^{n} a_{n-i} u^i v^{n-i} \quad . \tag{1}$$

The use of homogeneous variables corresponds to the substitution $x = u/v$.

Now consider the projection of points on the Riemann sphere onto its equatorial plane, taken as an Argand plane as noted above (Figure 2). A complex number $z = a + bi$ gives

$$a = \frac{p}{1-r} \quad , \quad b = \frac{q}{1-r} \quad , \quad a + bi = \frac{p + iq}{1-r} \quad . \tag{2}$$

Solving for p, q, and r gives

$$p = \frac{2a}{1 + a^2 + b^2} \quad , \quad q = \frac{2b}{1 + a^2 + b^2} \quad , \quad r = \frac{-1 + a^2 + b^2}{1 + a^2 + b^2} \quad . \tag{3}$$

Every rotation of the Riemann sphere around its center corresponds to a linear substitution

$$z' = \frac{\alpha z + \beta}{\gamma z + \delta} \quad . \tag{4}$$

For a rotation of the sphere by an angle θ where p, q, r and $-p$, $-q$, $-r$ remain constant,

$$z' = \frac{(v + iu)z - (t - is)}{(t + is)z + (v - iu)} \tag{5}$$

where $s = p \sin(\theta/2)$, $t = q \sin(\theta/2)$, $u = r \sin(\theta/2)$, and $v = \cos(\theta/2)$ so that

$$s^2 + t^2 + u^2 + v^2 = 1 \quad . \tag{6}$$

For a rotation about the polar axis this reduces to

$$z' = e^{i\theta} z \quad . \tag{7}$$

Now consider the vertices of a regular octahedron and a regular icosahedron as points on the surface of such a Riemann sphere oriented such that the north pole ($z = \infty$) is one of the vertices in each case. This leads to the following homogeneous polynomials for these regular polyhedra in these orientations where z is taken to be u/v.[18,19]

(a) Octahedron (O_h symmetry):

$$\text{Vertices: } \tau = uv(u^4 - v^4) \tag{8a}$$

$$\text{Edges: } \chi = u^{12} - 33u^8v^4 - 33u^4v^8 + v^{12} \tag{8b}$$

$$\text{Faces: } W = u^8 + 14u^4v^4 + v^8. \tag{8c}$$

(b) Icosahedron (I_h symmetry):

$$\text{Vertices: } f = uv(u^{10} + 11u^5v^5 - v^{10}) \tag{9a}$$

$$\text{Edges: } T = u^{30} + 522u^{25}v^5 - 10{,}005u^{20}v^{10} - 10{,}005u^{10}v^{20} - 522u^5v^{25} + v^{30} \tag{9b}$$

$$\text{Faces: } H = -u^{20} + 228u^{15}v^5 - 494u^{10}v^{10} - 228u^5v^{15} - v^{20} \quad . \tag{9c}$$

In order to generate similar polynomials for a regular tetrahedron, align a tetrahedron on the Riemann sphere so that the midpoints of its six edges are the same as the vertices of the octahedron defined by the polynomials (8a–8c). Then the tetrahedral polynomials are the following:

$$\text{Vertices: } \Phi = u^4 + 2\sqrt{-3}\cdot u^2v^2 + v^4 \tag{10a}$$

$$\text{Edges: } \tau = uv(u^4 - v^4) \qquad \text{(same as equation 8a)} \tag{10b}$$

$$\text{Faces: } \psi = u^4 - 2\sqrt{-3}\cdot u^2v^2 + v^4 \ . \tag{10c}$$

The roots of these polyhedral polynomials correspond to the locations of the vertices, edge midpoints, and face midpoints on the Riemann sphere. For example, the six roots of the vertex polynomial of the octahedron (equation 8a) are ∞, 0, ± 1, and $\pm i$, which are the locations of the six vertices of the octahedron on the Riemann sphere. The root of ∞ for equation (8a) relates to the absence of a u^6 or v^6 term even though all of the terms are of degree 6 implying the need for six roots.

The degrees of the polyhedral polynomials are equal to the numbers of corresponding elements (vertices, edges, or faces). Furthermore, interchanging the vertex and face polynomials for a given polyhedron gives the corresponding polynomials for its dual. For example, since the dual of an octahedron is a cube, the vertex polynomial of the octahedron (equation 8a) is the face polynomial of the dual cube and the face polynomial of the octahedron (equation 8c) is the vertex polynomial of the dual cube. Also since the tetrahedron and its dual, also a tetrahedron, together form a cube, the product of the vertex and face polynomials of a tetrahedron (*i.e.*, equations 10a and 10c) equals the vertex polynomial of the cube or the face polynomial of its dual, namely the octahedron (equation 8c).

The concept of a Riemann surface was originally introduced to facilitate the integration of multi-valued functions.[17] A simple example of such a multi-valued function is the function $w = \sqrt{z}$ which has two values depending on whether the positive or negative square root is taken. However, in order to illustrate the geometry of Riemann surfaces it is instructive to use the more complicated function

$$w = \sqrt{a_4z^4 + a_3z^3 + a_2z^2 + a_1z + a_0} \tag{11a}$$

$$\Rightarrow w = \sqrt{a_4(z - z_1)(z - z_2)(z - z_3)(z - z_4)} \tag{11b}$$

in which $a_0,\ldots,a_4$ are arbitrary complex constants and $z_1,\ldots,z_4$ are the roots of the polynomial under the radical. If z is a complex variable, such as that represented on the surface of a Riemann sphere, then equation (11) defines

w as a two-valued algebraic function of z. This equation is used to define a so-called elliptic curve,[20] where a point on the elliptic curve is a pair (z,w) satisfying equation (11).

The value of w in equation (11) might appear to depend upon five variables, either a_n $(0 \le n \le 4)$ in equation (11a) or a_4 and z_n $(1 \le n \le 4)$ in equation (11b). However, for the purpose of integration to give, for example, an elliptic integral, this function actually depends on only one complex variable, which is called the cross-ratio, λ.[20,21] Thus consider

$$z' = \frac{(z - z_4)(z_3 - z_2)}{(z - z_2)(z_3 - z_4)} \quad . \tag{12}$$

Equation (12) takes z_1 to

$$z_1 \to \frac{(z_1 - z_4)(z_3 - z_2)}{(z_1 - z_2)(z_3 - z_4)} = \frac{1}{\lambda} \tag{13}$$

in which

$$\lambda = \frac{(z_1 - z_2)(z_3 - z_4)}{(z_1 - z_4)(z_3 - z_2)} \quad . \tag{14}$$

Equation (12) also takes z_2 to ∞, z_3 to 1, and z_4 to 0. Now solve for z as a function of z' and substitute for z in the right hand side of equation (11) to give

$$\left[1 - z'\left(\frac{z_3 - z_4}{z_3 - z_2}\right)\right]^4 w^2 = a_4' z'(1 - z')(1 - \lambda z') \tag{15}$$

in which

$$a_4' = (z_2 - z_4)^2 (z_3 - z_4)^2 \left(\frac{z_1 - z_4}{z_3 - z_2}\right) a_4 \quad . \tag{16}$$

Now let

$$\left[1 - z'\left(\frac{z_3 - z_4}{z_3 - z_2}\right)\right]^2 w = w' \tag{17}$$

so that

$$w'^2 = a_4' z'(1 - z')(1 - \lambda z') \quad . \tag{18}$$

Next let

$$w'' = \frac{2w'}{\sqrt{a_4'}} \tag{19}$$

so that

$$w''^2 = 4z'(1 - z')(1 - \lambda z') \quad . \tag{20}$$

Dropping all primes from equation (20) gives the elliptic curve in the Riemann normal form, *i.e.*

$$w^2 = 4z(1-z)(1-\lambda z) \quad . \tag{21}$$

Thus given equation (11) of an elliptic curve, the Riemann normal form (equation 21) can be obtained by computing the cross-ratio, λ, of the four roots of the polynomial. Note that in converting equation (11) to equation (21) the degree of the polynomial in z on the right hand side is reduced from 4 to 3 corresponding to sending one root of the quartic in (11) to infinity in the transformation of equation (11) to equation (21).

With this algebraic background the Riemann surface can be obtained corresponding to the Riemann normal form (equation 21). The original purpose of the Riemann surface was to convert a multi-valued integrand, such as one containing a square root of a polynomial, into a single valued integrand in order to facilitate subsequent integration. In this connection note that in equation (11) for $z \neq z_1,\ldots,z_4$ there are two values of w corresponding to the positive and negative square roots. At $z_1,\ldots,z_4$, which are called critical points, there is a unique value for w, since the two values for w coalesce at these points.

We can construct a Riemann surface, M^2, for the elliptic curve represented by equation (21), which has critical points at 0, 1, $1/\lambda$, and ∞.[17] For convenience in obtaining M^2, we take the Argand plane (Figure 2) and slit it along the real axis from 0 to 1 and along a half line parallel to the real axis going to the right beginning at $1/\lambda$ and ending at ∞ (Figure 3). An important requirement in slitting the Argand plane is that the two slits do not intersect. To represent w defined by equation (21) in its entirety, we take a second copy of the slit Argand plane and attach this second copy to the first at the points 0, 1, $1/\lambda$, and ∞ and along the slits. The bottom of each slit on either sheet is attached to the top of the corresponding slit on the other sheet, where a sheet refers to a single copy of the Argand plane. The two sheets can thus be pictured as being parallel and lying over the Argand plane so that each point projects down vertically on the point of the Argand plane with the same value of z. Since each of the two slit sheets may be mapped onto a sphere, the Riemann surface M^2 is like a basketball and an internal air bladder joined by the two crossed slits.

Surfaces, including Riemann surfaces such as the one described above, can be characterized by their genus. The genus of a sphere or a surface topologically homeomorphic to a sphere is zero. In this connection two surfaces S_1 and S_2 are said to be topologically homeomorphic to each other if S_1 can be deformed to S_2 without tearing or cutting. Surfaces of non-zero genus are topologically homeomorphic to surfaces generated by drilling holes (or tun-

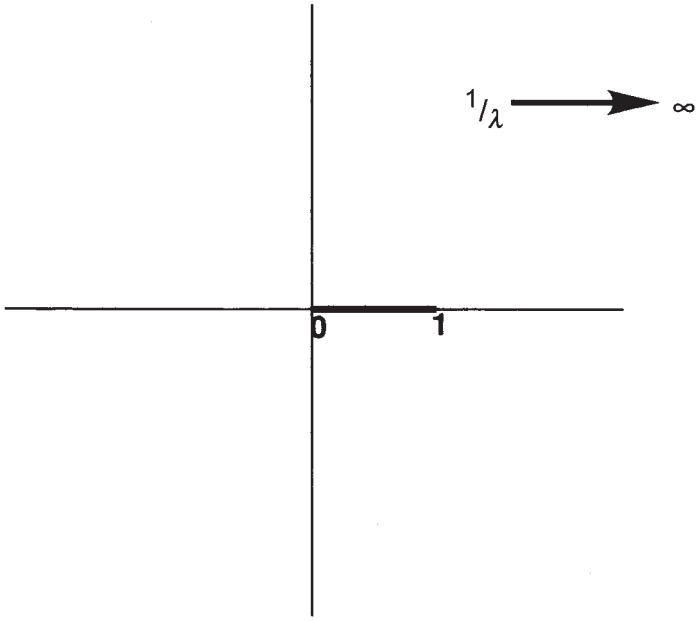

Figure 3. A sheet of the Riemann surface for the equation $w^2 = 4z(1 - z)(1 - \lambda z)$ (equation 21). In Figures 3, 7, and 8 depicting sheets of Riemann surfaces, bold lines, arrows, or curves indicate the locations of the slits.

nels) through a plastic sphere. The genus, g, of such a surface is the number of holes that must be drilled through a plastic sphere to make a surface homeomorphic to the surface in question. Thus the genus of a sphere itself is zero and the genus of a torus (*i.e.*, a doughnut) is one. Note that a standard coffee cup with one handle and a doughnut are both examples of surfaces of genus one. The Riemann surface for equation (13) is also an example of a surface of genus one.[17] We will find that the Riemann surfaces of interest in connection with study of the Klein and Dyck tessellations both have genus three.

PLATONIC TESSELLATIONS OF RIEMANN SURFACES

The Riemann surfaces used to model allotropes of carbon and boron nitride with structures based on IPMS's may be considered to be decorated or tessellated with polygons corresponding to the fused rings of the atoms making up the chemical structure in question. For example, in the D168 structure for a carbon allotrope, the genus three surface is tessellated with hexagons and heptagons corresponding to the C_6 and C_7 carbon rings in the

structure. In this connection a tessellation of a surface can be described in terms of its flags, where a flag is a triple (V, E, F) consisting of a vertex V, an edge E, and a face F, which are mutually incident.[22] A tessellation is called platonic if its symmetry group acts transitively on its flags. The regular polyhedra (Figure 1) are examples of platonic tessellations of the sphere. The so-called Schäfli notation $\{p,q\}$ can describe a platonic tessellation consisting of q regular p-gons at each vertex.

Now consider platonic tessellations in the Euclidean plane, *i.e.*, a flat surface of zero curvature. In the Euclidean plane, the angle of a regular p-gon $\{p\}$, is $(1 - 2/p)\pi$; hence q equal $\{p\}$'s of any size will fit together around a common vertex if this angle is equal to $2\pi/q$ leading to the following relationship:

$$(p - 2)(q - 2) = 4 \quad . \tag{22}$$

There are only three integral solutions of equation (22), which lead to the three platonic tessellations of the plane, namely {4,4}, {6,3}, and {3,6} (Figure 4). The {4,4} tessellation is the pattern of the checkerboard and the {6,3} tessellation corresponds to the structure of graphite.

Now consider platonic tessellations of the sphere that correspond to the regular polyhedra (Figure 1). The angle of the regular spherical polygon $\{p\}$ is greater than $(1 - 2/p)\pi$ and gradually increases from this value to π as the circumradius of the underlying sphere increases from 0 to $\pi/2$. Thus if

$$(p - 2)(q - 2) < 4 \quad , \tag{23}$$

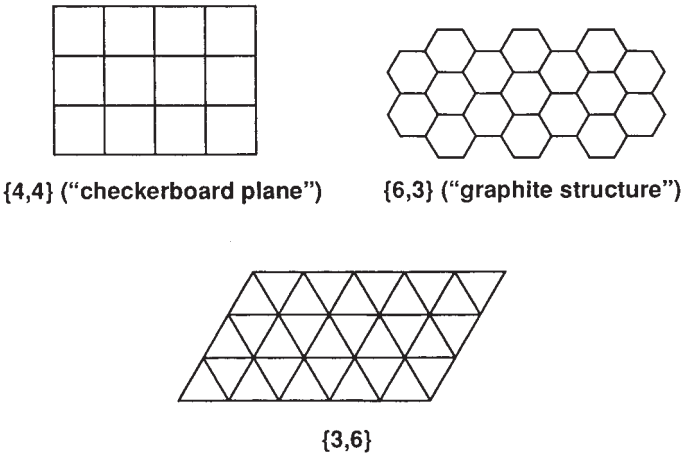

Figure 4. The three platonic tessellations of the plane.

then the size of $\{p\}$ can be adjusted so that its angle is exactly $2\pi/q$. Then q such $\{p\}$'s will fit together around a common vertex leading to the platonic spherical tessellations $\{2,q\}$, $\{p,2\}$, $\{3,3\}$, $\{3,4\}$, $\{4,3\}$, $\{3,5\}$, $\{5,3\}$ corresponding to the q-gonal hosohedron formed by q lunes,[23] the p-gonal dihedron formed by two p-gons, the regular tetrahedron, the regular octahedron, the cube, the regular icosahedron, and the regular dodecahedron, respectively (Figure 1). In this connection a lune is a spherical polygon with two vertices and two edges.

Finally consider regular tessellations in the hyperbolic plane, in which the angle of a regular hyperbolic polygon $\{p\}$ is less than $(1 - 2/p)\pi$ and gradually decreases from this value to zero when the (negative) curvature goes from 0 to $-\infty$. Thus if

$$(p - 2)(q - 2) > 4 \ , \tag{24}$$

then the size of $\{p\}$ can be adjusted so that its angle is exactly $2\pi/q$. Then q such $\{p\}$'s will fit together around a common vertex and further $\{p\}$'s may be added indefinitely. In this manner, a regular hyperbolic tessellation $\{p,q\}$ can be constructed, which is an infinite collection of regular p-gons filling the whole hyperbolic plane. There are obviously an infinite number of integral solutions to equation (22) leading to an infinite number of different regular hyperbolic tessellations. The regular hyperbolic tessellations $\{7,3\}$ and $\{8,3\}$ correspond to the genus 3 Klein and Dyck tessellations, respectively, which are the ones of interest in the context of this paper. For convenience in some of the figures the edges of the hyperbolic polygons are drawn as straight lines even though they are actually curved lines.

Euler's theorem can be generalized to tessellations embedded in a surface of genus g (or Euler characteristic χ) by using the following equation:

$$v - e + f = 2(1 - g) = \chi \ . \tag{25}$$

Note that if $g = 0$ so that $\chi = 2$ (*i.e.*, for polyhedra homeomorphic to a sphere), equation (25) reduces to the familiar version of Euler's theorem, *i.e.*

$$v - e + f = 2 \ . \tag{26}$$

Platonic tessellations of surfaces with constant curvature can be constructed by reflections in three mirrors defined by three sides of a right triangle of geodesics, called an orthoscheme triangle or asymmetric unit (Figure 5a).[24,25] The orthoschemes correspond to the flags of the tessellation. For a platonic tessellation $\{p,q\}$ the acute angles of the orthoscheme are π/p and π/q. The set of replicas of one orthoscheme obtained by repetitions of

these reflections covers the surface totally without overlap. For example, in the Euclidean plane, the {6,3} and {3,6} platonic tessellations of hexagons and triangles (Figure 4) are obtained from an orthoscheme with angles of $\pi/2$, $\pi/6$, and $\pi/3$. Similarly, the {4,4} checkerboard tessellation of squares is obtained from an orthoscheme with angles of $\pi/2$, $\pi/4$, and $\pi/4$. Furthermore, on the sphere, each of the regular polyhedra (Figure 1) can be obtained from its own orthoscheme. For example, a regular dodecahedron {3,5}, as well as its dual icosahedron {5,3}, can be generated from a non-Euclidean orthoscheme with angles of $\pi/2$, $\pi/3$, and $\pi/5$. Figure 5b shows the division of a single pentagonal face of a regular dodecahedron (Figure 1) into ten of these orthoschemes, alternately shaded and unshaded. Extension of this division to all 12 faces of the regular dodecahedron leads to a total of 120 orthoschemes to cover the entire surface of the regular dodecahedron. The orthoscheme triangle is the fundamental region of the symmetry (automorphism) group of the tessellation. Two points of the same fundamental region are not related by a symmetry operation and all points related by a symmetry operation are equivalent to one point of the orthoscheme. In the example of the regular dodecahedron the 120 orthoschemes represent the 120 operations of the full icosahedral symmetry group I_h. Similarly the 60 unshaded orthoschemes (or equivalently the 60 shaded orthoschemes) represent the 60 proper rotations of the icosahedral rotational subgroup I.

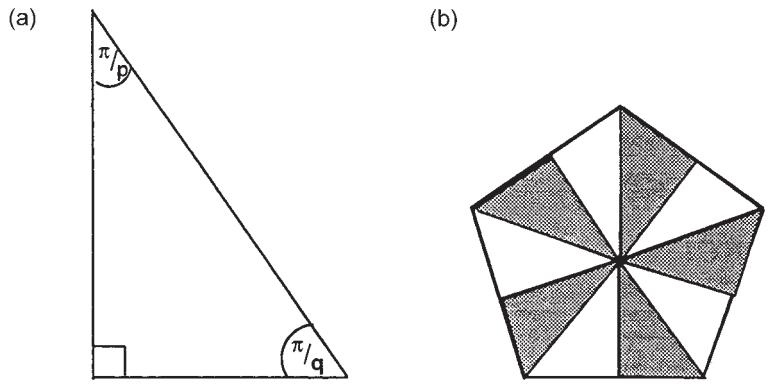

Figure 5: (a) An orthoscheme triangle for the platonic tessellation $\{p,q\}$. (b) Division of one of the 12 pentagonal faces of the regular dodecahedron into its 10 orthoscheme triangles showing the alternate shaded and unshaded triangles.

The conversion of platonic tessellations into favorable structures for carbon and boron nitride allotropes requires the use of a so-called leapfrog transformation to introduce hexagonal rings in a symmetrical manner.[8–12]

The leapfrog transformation of a tessellation consists of omnicapping (stellation) followed by dualization (Figure 6) and the final tessellation is called the leapfrog of the original tessellation. This reduces considerably the angular strain thereby generating an energetically favorable structure. Leapfrog transformations have the following characteristics:

(1) In the leapfrog transformation of a trivalent tessellation (*i.e.*, one with a Schäfli symbol of the type $\{3,q\}$) the numbers of vertices and edges are triple the numbers of vertices and edges, respectively, in the original tessellation.

(2) The number of faces in the leapfrog of a trivalent tessellation is equal to the sum of the numbers of vertices and faces in the original tessellation.

(3) The permutational symmetry (*i.e.*, the point group symmetry in the case of the genus zero polyhedra) of the original tessellation is retained in the leapfrog.

(4) The leapfrog transformation of a trivalent tessellation »dilutes« the original tessellation with the minimum number of hexagons so that no two polygons from the original tessellation share a common vertex or edge in the leapfrog. Furthermore, each vertex of the leapfrog belongs to exactly one polygon from the original tessellation.

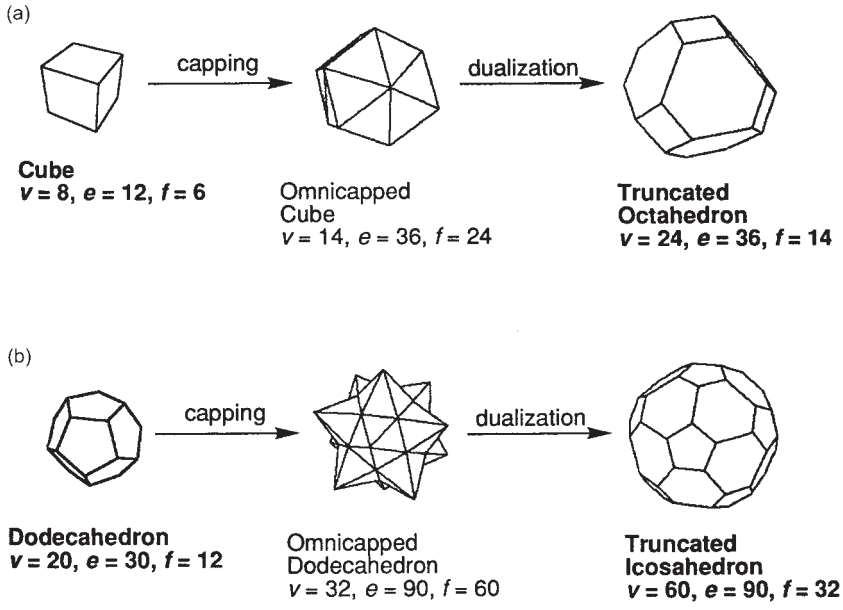

Figure 6. (a) Leapfrog transformation of the cube into the truncated octahedron. (b) Leapfrog transformation of the regular dodecahedron into the truncated icosahedron (C_{60} polyhedron).

The most familiar example of a leapfrog transformation is the conversion of the 20-vertex regular dodecahedron into the 60-vertex truncated icosahedron of C_{60}. Similarly the D168 structure for the hypothetical Vanderbilt-Tersoff allotrope of carbon[5] consisting only of hexagons and heptagons can be obtained by a leapfrog transformation from the Klein tessellation.[6]

A GENUS 2 RIEMANN SURFACE OF PENTAGONAL BIPYRAMIDAL SYMMETRY

Before considering the genus 3 Riemann surfaces corresponding to the Klein and Dyck tessellations, it is first instructive to consider a simpler Riemann surface B^2 consisting of a genus 2 surface tessellated by F equilateral $\pi/5$ triangles (*i.e.*, triangles in which each angle is $\pi/5$).[26] In order for such a triangular tessellation (triangulation) to be platonic, it must have $E = \frac{3}{2}F$ edges and $V = \frac{3}{10}F$ vertices, since ten triangles meet at a vertex. Solving for $\chi(B^2)$ in Euler's formula (equation 25) gives the following:

$$\chi(B^2) = V - E + F = F \cdot \left(\frac{3}{10} - \frac{3}{2} + 1 \right) = -2 \ . \tag{27}$$

Equation (27) leads to $F = 10$, $E = 15$, and $V = 3$. The ten triangles fitting around one vertex form a $2\pi/5$ decagon, which is a fundamental domain for a surface that we want to construct (Figure 7a). What remains is the derivation of suitable identifications of edges of the decagon to generate a quotient surface with the necessary conditions for a platonic tessellation. For example, we want the $2\pi/5$ rotations around the center of the decagon to extend to permutational symmetries of the surface. This implies that identification of one pair of edges determines all of the other edge identifications. Since the angles at five decagon vertices sum to 2π, the edge identifications have to identify every second vertex. This leaves only the two possibilities of identifying edges 1 and 4 and identifying edges 1 and 6. Both are seen to lead to the same Riemann surface, which has genus 2.

The quotient surfaces can be defined algebraically by constructing two meromorphic functions and determining the algebraic relationship between them. To define the first such function, z, consider the C_5 rotation group around the center of the decagon. This group has three fixed points, namely the center of the decagon and the two identified sets of vertices. Using Euler's formula (equation 25) the quotient surface can be seen to be a sphere. Thus take any triangulation of B^2 that is invariant under the rotation group. Then the quotient surface is also triangulated. If the number of fixed points of the rotations on M^2 is f, then the Euler number can be computed

for this quotient surface by the following equation derived from equation (25):

$$\frac{1}{5}[(V-f)-E+F]+f=\frac{1}{5}(-2-f)+f\in\{0,2\}\quad . \tag{28}$$

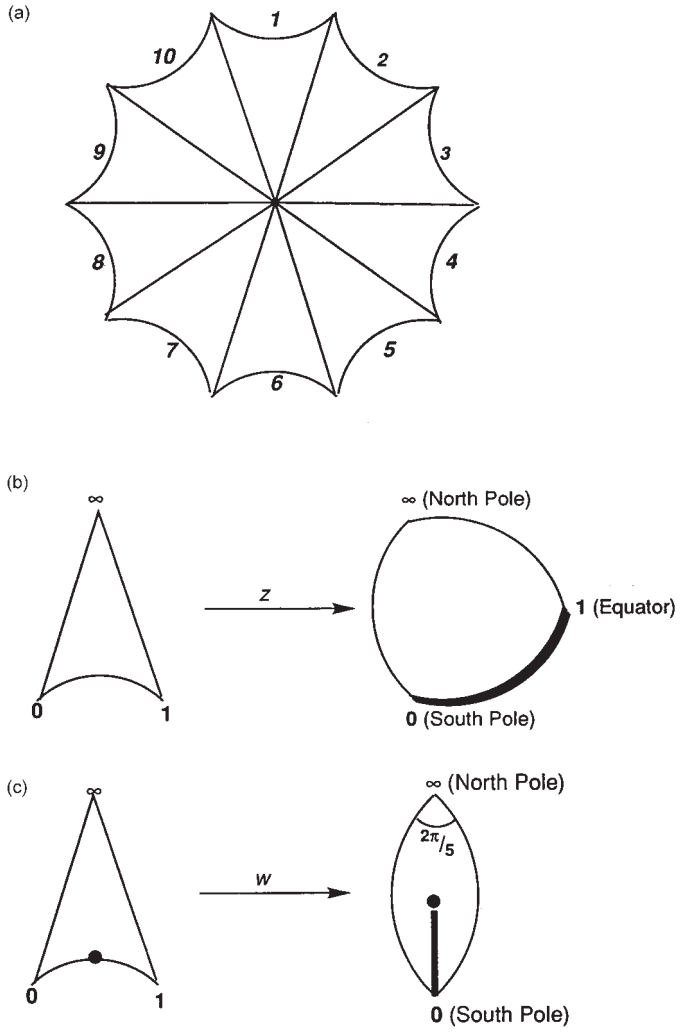

Figure 7. (a) Division of the $2\pi/5$ decagon representing the genus 2 Riemann surface B^2 into 10 equivalent triangles. In Figures 7, 8, and 10 the edges are labeled by italic numbers. (b) The function z arising from mapping one of the triangles onto half of the Riemann sphere with a slit from 0 to 1. (c) The function w arising from mapping one of the triangles onto one-fifth of the Riemann sphere with a slit bisecting the angle at 0.

This indicates that $f = 3$ and shows that for this quotient surface $\chi = 2$ corresponding to a sphere. The coefficient 1/5 in equation (28) relates to the fact that the C_5 rotation group effectively »divides« B^2 by five.

An alternative method for studying this Riemann surface uses what is called Riemann mapping. Color the ten triangles in Figure 7a alternately black and white. »Riemann map« a white triangle to the upper hemisphere of the Riemann sphere (Figure 2). »Möbius normalize« the Riemann sphere so that the vertices of the triangle go to 0, 1, and ∞ and extend analytically by reflection in the radial boundary to a map from the decagon to a fivefold covering of the sphere branched over ∞ and with slits from 0 to 1 on each sheet. Finally identify the edges of the slits in the same way as the pre-image edges of the decagon. The quotient sphere is thus seen as isometric to the double of a hyperbolic $2\pi/5$ triangle. Alternatively the Riemann surface B^2 can be seen as a fivefold covering of the Riemann sphere, branched over 0, 1, ∞. In any case this leads to a meromorphic function z on M^2 that sends the three vertices of the triangulation as fivefold branch points to 0, 1, and ∞ (Figure 7b).

In order to define the second function, w, consider the quotient of B^2 by any involution (symmetry operation of period 2) to give the following equation where B^2 is effectively »divided« by two:

$$\frac{1}{2}[(V-f)-E+F]+f=\frac{1}{2}(-2-f)+f\in\{0,2\}\quad . \tag{29}$$

This leads to $f = 2$ or $f = 6$. In both cases the involution taken is the one used to define the identifications leading to the solution $f = 6$ corresponding to $\chi = 2$ and a sphere. The resulting meromorphic function w on M^2 is normalized by sending the midpoint of the decagon to ∞ and the two other vertices of the triangulation to 0. Since reflection in the triangle edges corresponding to radii of the decagon passes to the quotient, the function w can also be understood as mapping each triangle to a spherical $2\pi/5$ sector that is bounded by great circle arcs from 0 to ∞ and has a straight slit in the direction of the angle bisector (Figure 7b). By scaling the slit may be taken to arbitrary length.

By comparing the divisors of z and w we see that w^5 and $z(z-1)$ are proportional and can be scaled so that

$$w^5 = z(z-1). \tag{30}$$

The multi-valued nature of w can be emphasized by rewriting equation (30) as

$$w=\sqrt[5]{z(z-1)} \tag{31}$$

corresponding to the five-fold covering of the Riemann sphere by the quotient Riemann surface corresponding to $z(z-1)$. Also note that equations (30) or (31) are defining equations for B^2 for either identification pattern, *i.e.*, edge 1 to edge 4 and edge 1 to edge 6 (Figure 7a).

This triangle tessellation is seen not to be platonic since if it were platonic the 120° rotation of one triangle would extend to a symmetry of the whole surface. The symmetry of this tessellation is thus limited to the same D_5 pure rotation group of the pentagonal bipyramid, which like the original tessellated decagon (Figure 7a) has 10 triangular faces. The two equivalent right triangles obtained by bisecting each of the 10 triangular faces of the tessellated decagon in a manner to preserve the D_5 symmetry lead to 20 orthoschemes which correspond to the 20 operations of the D_{5h} point group of the pentagonal bipyramid.

GENUS 3 RIEMANN SURFACES: THE KLEIN AND DYCK TESSELLATIONS

The Klein Tessellation

The Klein tessellation, K^2, is a {3,7} tessellation of a genus 3 surface by $2\pi/3$ regular heptagons. If F is the number of faces of such a tessellation, the number of vertices V is $\frac{7}{3}F$ and the number of edges E is $\frac{7}{2}F$ so that Euler's formula (equation 25) gives the following result:

$$\chi(K^2) = -4 = F\cdot\left(1-\frac{7}{2}+\frac{7}{3}\right) \Rightarrow\ F = 24, \quad V = 56, \quad E = 84. \tag{32}$$

In the dual {7,3} tessellation of the genus 3 surface by $2\pi/7$ triangles (the little triangles) the numbers F and V are interchanged. The leapfrog of K^2 has $3V = 168$ vertices, $3E = 252$ edges, and $F + V = 80$ faces (56 hexagons and 24 heptagons) corresponding to a unit cell of the D168 structure for a carbon allotrope suggested by Vanderbilt and Tersoff.[5]

Consideration of the properties of the Klein tessellation, K^2, is facilitated by considering a coarser tessellation, M^2, of the same genus 3 surface by big triangles so that six small triangles of K^2 make up each big triangle of M^2. The coarse tessellation M^2 (Figure 8a) has fourteen $\pi/7$ triangles so oriented to have a cyclic group of order 7 (C_7) as at least part of its automorphism group. Euler's theorem requires M^2 to have 21 edges and 3 vertices. There are two distinct genus 3 Riemann surfaces of this type but only one of these two has the 120° rotations (C_3 operations) around triangle centers as part of its automorphism group. This latter Riemann surface is the one used

to generate K^2 by subdividing each of its big triangles into six of the little triangles of K^2.

Now consider a cyclic rotation group of prime order p on a surface of genus 3 with f fixed points. The Euler number for the quotient surface obtained by »division« by p is given by the following equation:

$$\frac{1}{p}[(V-F)-E+F]+f=\frac{1}{p}(-4-f)+f\in\{-2,0,2\} \tag{33}$$

so that

$$f\in\left\{-2+\frac{2}{p-1},\ \frac{4}{p-1},\ 2+\frac{6}{p-1}\right\} \tag{34}$$

is an integer for $\chi = \{-2,0,2\}$, respectively.

Therefore $p = 7$ is the maximum prime order, $f = 3$ in that case, and the quotient surface is a sphere, *i.e.*, of genus 0 with $\chi = 2$. A genus 3 surface with an order 7 cyclic group of automorphisms therefore has a natural quotient map to the sphere. This quotient map may be mapped onto the Riemann sphere by sending the three fixed points to 0, 1, and ∞.

Equation (34) also shows that an involution (*i.e.*, an operation of period 2) must have $f = 0$, 4, or ∞ fixed points for quotient surfaces of genera 0, 1, and 2, respectively. However, an involution of a platonic {3,7} tessellation cannot have its fixed points at the vertices or the centers of the faces of the tessellation. Thus the fixed points of the involutions must be at edge midpoints. In such a case f must divide the number E of edges. Therefore $f = 8$, which corresponds to a genus 0 quotient surface, cannot occur for an involution of the Klein tessellation K^2 with 84 edges. The quotient surface for an involution of a platonic tessellation of heptagons thus cannot be a sphere but must be a torus.

A platonic {3,7} tessellation also implies a rotation group of order $p = 3$ around each of the heptagon vertices. Equation (34) for $p = 3$ indicates that the number of fixed points, f, must be 2 or 5 for genus 1 and 0, respectively. However $f = 5$ is excluded since it does not divide $V = 56$. Therefore f must be 2 corresponding to a torus of genus 1 for a quotient surface for a rotation group of order 3.

Now consider the coarser tessellation, M^2, of the 14 big triangles to form a hyperbolic tetradecagon (Figure 8a). We see that all of the odd and all of the even vertices each have to be identified separately to give a smooth hyperbolic surface with the required 3 vertices. This leaves three possibilities: identify edge 1 to edge 4, 6, or 8. The last case has the 180° rotation around the center of the tetradecagon as an involution with $f = 8$ fixed points (na-

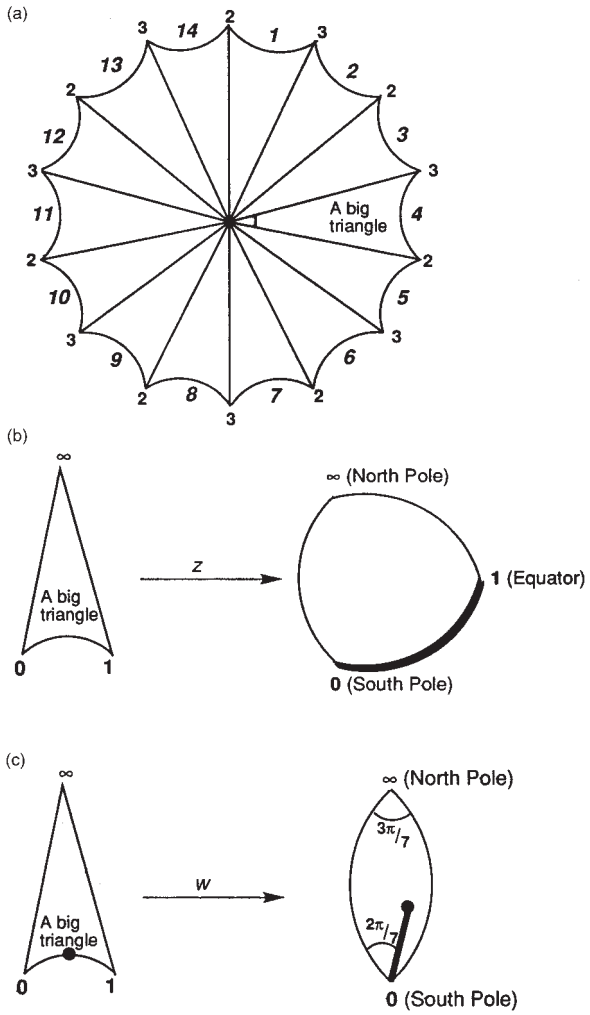

Figure 8: (a) The coarse tessellation M^2 of a tetradecagon representing the genus 3 Klein tessellation K^2 into 14 equivalent big triangles. The italic numbers on the outer edges can also be considered as numbers of the corresponding triangles. (b) The function z arising from mapping one of the big triangles onto one-half of the Riemann sphere with a slit from 0 to 1. (c) The function w arising from mapping one of the big triangles onto 3/14 of the Riemann sphere with a slit dividing the $3\pi/7$ angle at 0 into angles of $\pi/7$ and $2\pi/7$.

mely the center and the pairwise-identified midpoints of the tetradecagon edges) so that the quotient surface is a sphere and thus M^2 is not platonic. Identification of edge 1 to 4 leads to the same genus 3 surface thereby leaving only the identification of edge 1 to edge 6 as a candidate for a platonic

surface. This latter identification turns out to be the coarse tessellation, M^2, corresponding to the Klein tessellation, K^2, and is consistent with Klein's original description of this tessellation.[7]

The proof of platonicity of Klein's tessellation, K^2, can use the coarse tessellation M^2 (Figure 8a) with the 14 big triangles colored alternately black and white to show that the 120° rotations (C_3) in the center of each big triangle are part of the automorphism group. In Figure 8a the odd-numbered edges can be assumed to be black and the even-numbered edges to be white. In the identification of edge 1 to edge 6 each black edge of the tetradecagon is identified with the white edge that is counterclockwise 5 steps ahead (or the white edges with the black ones 9 steps ahead). Now call the vertex at the center of the tetradecagon vertex 1, the left endpoint of a black edge vertex 2 and its right endpoint vertex 3. The identification of edge 1 to edge 6 can be restated as follows:

(1) Vertex 2 as seen from vertex 1 is rotated by $2 \cdot 2\pi/7$ around the center of the tetradecagon.

(2) The triangle adjacent to this black edge is, at vertex 2, rotated by $1 \cdot 2\pi/7$.

(3) Vertex 3 is rotated by $3 \cdot 2\pi/7$ around the center of the tetradecagon.

(4) The same triangle adjacent to this black edge is rotated around vertex 3 by $-1 \cdot 2\pi/7$.

Thus rotation around vertex 1 by $2\pi/7$ is rotation at vertex 2 by $4 \cdot 2\pi/7$ and at vertex 3 by $2 \cdot 2\pi/7$. This rule remains the same (mod 7) if the vertices are cyclically permutated thereby demonstrating the three-fold symmetry of the coarse tessellation M^2 and hence the Klein tessellation, K^2.

In order to apply this identification rule, consider the coarse tessellation M^2 (Figure 8a) with the 14 $\pi/7$ big triangles alternately colored black and white. The equivalence classes of triangles and their vertices are marked from 1 to 14 and from 1 to 3, respectively. The 120° rotation around any triangle center cyclically permutes the (equivalence classes of) vertices. Similarly, reflection in a triangle edge interchanges the black and white triangles and therefore the cyclic orientation of their vertices. However, neither of these two operations changes the identification rule. These reflections generate the order 7 rotational symmetry and thus pass to the quotient sphere obtained by »dividing« by seven (see equations (33) and (34) for $p = 7$). This quotient sphere is generated by mapping a black triangle to the upper half plane and then normalizing the triangle so that vertices 3, 2, and 1 go to 0, 1, and ∞, respectively. This quotient sphere generates the function z for the Klein tessellation (Figure 8b).

The coarse tessellation M^2 can also be mapped onto a Riemann sphere in a second way to generate a function w. Thus map one of the black triangles

of M^2 to a spherical domain that is bounded by two great circles from 0 to ∞ with angle $3\pi/7$ at ∞. This sphere has a great circle slit from 0 dividing the angle at 0 in the ratio 2:1 with the bigger angle counterclockwise first (Figure 8c). This map can be extended analytically by reflection in the edges (around ∞) to cover the sphere three times. The slits in these three sheets are such that always in two sheets there are slits above each other, and these are not always above a slit in the third sheet. This forced identification of the slits is compatible with the identification of the edges of the tetradecagon since the rotation angles $\{4,1,2\}\cdot 2\pi/7$ counterclockwise at the vertices of a black triangle are the same as the rotation angles $\{-3,1,2\}\cdot 2\pi/7$ at the vertices of the Riemann sphere. By comparing the divisors of w and the above quotient function z we find that w^7 and $z(z-1)^2$ are proportional and can be scaled to give the following equation:

$$w^7 = z(z-1)^2 \tag{35a}$$

$$w = \sqrt[7]{z(z-1)^2} \quad . \tag{35b}$$

Now introduce the new variables x and y defined by the equations:

$$x = \frac{-(1-z)}{w^2} \tag{36a}$$

$$y = \frac{(1-z)}{w^3} \quad . \tag{36b}$$

Solving equations (36) for w and z gives the following:

$$w = -x/y \tag{37a}$$

$$z = 1 + \frac{x^3}{y^2} \quad . \tag{37b}$$

Substituting equations (37) into equation (35) gives

$$x^3y + y^3 + x = 0 \quad . \tag{38}$$

Introducing the homogeneous variables $x = \xi/\omega$ and $y = \eta/\omega$ leads finally to the following homogeneous quartic equation:

$$\xi^3\eta + \eta^3\omega + \omega^3\xi = 0. \tag{39}$$

Equation (39) is unchanged upon permutation of the coordinates ξ, η and ω corresponding to the three-fold symmetry of the genus 3 Klein tessellation.

We will now generate the orthoschemes for the Klein tessellation in order to observe its automorphism group. Each of the 24 heptagons of the Klein tessellation can be divided into fourteen equivalent hyperbolic right triangles with angles of $\pi/2$, $\pi/3$, and $\pi/7$ (Figure 9a) leading to a total of $(14)(24) = 336$ orthoscheme triangles (Figure 9b). These orthoschemes can be divided into two equivalent sets (indicated in Figure 9b as shaded and unshaded triangles). Either set of orthoschemes corresponds to the 168 operations of the heptakisoctahedral group, ${}^7O$. Furthermore, the full set of 336 orthoschemes (shaded and unshaded) corresponds to the full group ${}^7O_d$ (Ref. 13). The latter group is generated from ${}^7O$ by addition of reflection operations and the improper rotation $S_6 = \sigma_v' \times C_7$ (Ref. 13). Six of the 336 orthoschemes make up the 56 (= 336/6) little triangles of the Klein tessellation and 24 of the 336 orthoschemes make up the 14 (= 336/24) big triangles of the tetradecagon (Figure 8a).

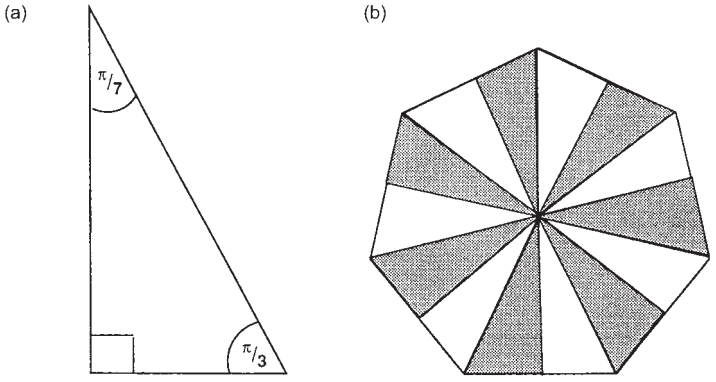

Figure 9. (a) The orthoscheme triangle for the Klein tessellation K^2. (b) Division of one of the 24 heptagonal faces of the Klein tessellation into its 14 orthoscheme triangles showing the alternate shaded and unshaded triangles.

The Dyck Tessellation

The Dyck tessellation, D^2, is generated by a {3,8} tessellation of a genus 3 surface by $2\pi/3$ octagons. If F is the number of faces of such a tessellation, the number of vertices V is $\frac{8}{3}F$ and the number of edges E is $\frac{8}{2}F = 4F$ so that Euler's formula gives the following result:

$$\chi(K^2) = -4 = F \cdot \left(1 - 4 + \frac{8}{3}\right) \Rightarrow F = 12, \quad V = 32, \quad E = 48. \tag{40}$$

In the dual {8,3} tessellation by $\pi/4$ triangles (*i.e.*, the little triangles in this case) the numbers F and V are interchanged. The leapfrog of D^2 has $3V = 96$ vertices, $3E = 144$ edges, and $F + V = 44$ faces (32 hexagons and 12 octagons).

Consideration of the properties of the Dyck tessellation, like those of the Klein tessellation, is facilitated by consideration of a coarser tessellation, M^2, consisting of eight $\pi/4$ hyperbolic squares fitting together around a central vertex to give a hexadecagon with vertex angles alternately $\pi/4$ and $2\pi/4$ (Figure 10a). Each of the eight $\pi/4$ hyperbolic squares in M^2 can be divided by a diagonal into two triangles to give a total of 16 triangles, namely

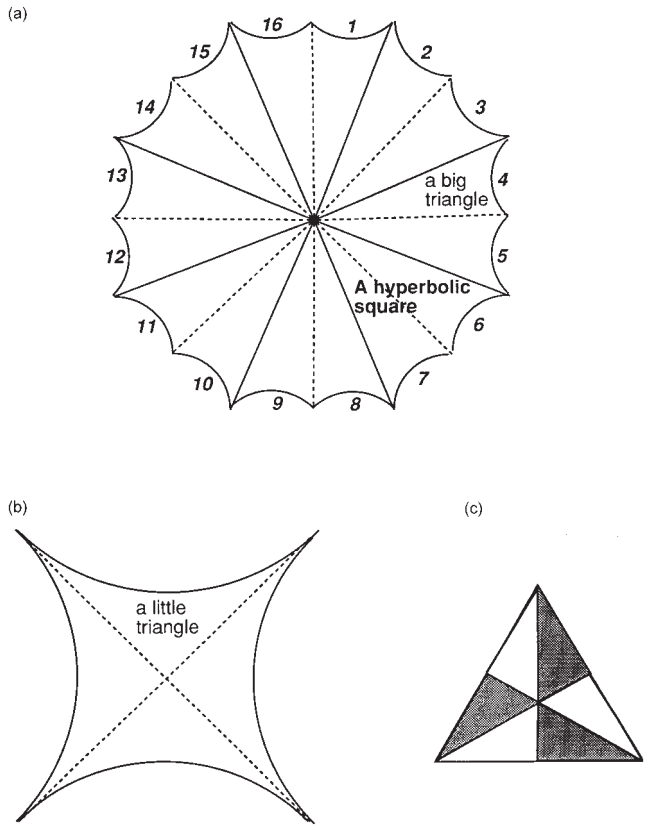

Figure 10: (a) The tessellation of a hexadecagon representing the genus 3 Dyck tessellation D^2 into 8 hyperbolic squares. One diagonal (dashed lines) divides each of the hyperbolic squares into two equivalent hyperbolic triangles, namely the big triangles of the coarse tessellation M^2. (b) Division of one of the 8 hyperbolic squares into four little triangles using both diagonals (dotted lines). (c) Division of one of the 32 little triangles into 6 orthoschemes.

the big triangles. Also both diagonals of a $\pi/4$ hyperbolic square divide the square into four little triangles (Figure 10b). Because of the alternating pattern of vertex angles, the only identification pattern consistent with platonicity has an edge from a $\pi/4$ vertex clockwise to a $2\pi/4$ vertex (*e.g.*, edge 1 in Figure 10a) identified with the edge five places away (edge 6 in Figure 10a). This identification pattern is that of the Dyck tessellation (Figure 11a).

Now consider the original Dyck tessellation of twelve octagons on the genus 3 surface. Take a given octagon, *e.g.*, octagon 1 in the center of Figure 11a, and inscribe two $\pi/4$ hyperbolic squares by joining even-numbered and odd-numbered vertices, respectively (Figure 11b). Extend one of these inscribed hyperbolic squares (called red) to a tessellation of the hyperbolic plane and color its tiles red and green in checkerboard fashion, *i.e.*, the {4,4} tessellation in Figure 4. Similarly, extend the other inscribed hyperbolic square (called blue) to another checkerboard tessellation, this time with blue/yellow tiles. These two complementary checkerboard tessellations can be colored so that they have the following properties:

(1) Each red tile has the same midpoint as a blue tile and each green tile has the same midpoint as a yellow tile.

(2) The vertices of the red/green tile are the midpoints of the yellow tiles and *vice versa*. Similarly the vertices of the blue/yellow tiles are the midpoints of the green tiles.

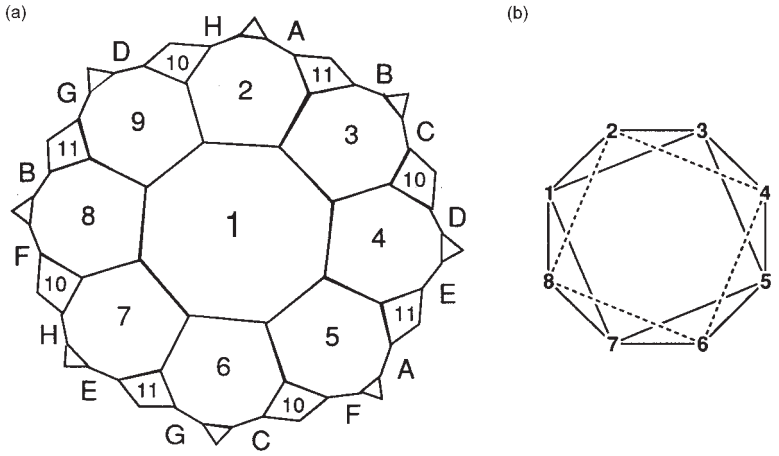

Figure 11. (a) The Dyck tessellation showing the twelve octagons and the pattern of identification of the outer edges. Thus in Figure 11a edges designed by the same letter, *i.e.*, A through H, are identified. (b) Inscription of two squares inside one of the octagons of the Dyck tessellation. Either square can be extended into a {4,4} tessellation, *i.e.* the checkerboard pattern.

Now define two functions f and g in this hyperbolic plane and consider their mapping onto the Riemann sphere (Figure 2). Map one tile to the unit disc of the Riemann sphere so that the vertices go to 1, i, –1, and –i, *i.e.*, the four fourth roots of 1. The functions f and g each have simple poles at the common centers of the red and blue squares, respectively. Furthermore each function has simple zeros at the other midpoints of its tiles, *i.e.*, at the four-fold branch points of the other function whose branch points are the fourth roots of –1. This leads to the following equation, known as the Fermat quartic:

$$f^4 + g^4 + 1 = 0. \tag{41}$$

Introducing the homogeneous variables ξ, η, and ω so that $f = \xi/\omega$ and $g = \eta/\omega$ leads to the following homogeneous quartic equation:

$$\xi^4 + \eta^4 + \omega^4 = 0. \tag{42}$$

If we now identify points on the hyperbolic plane that are not separated by f and g, we obtain a surface together with two tessellations by 8 squares. The vertices of both of the tessellations define a tessellation by 32 equilateral $\pi/4$ triangles. These 32 triangles correspond to the little triangles of the dual of the Dyck tessellation, namely the {8,3} tessellation. Each of these 32 little triangles (Figure 10b) are divided into six orthoschemes (Figure 10c) giving a total of $32 \times 6 = 192$ orthoschemes on the Dyck tessellation. If these 192 orthoschemes are shaded and unshaded in an alternating manner, the 96 orthoschemes of one type (either shaded or unshaded) generate the automorphism group of the Dyck tessellation, namely the tetrakisoctahedral group ${}^4O$. This group has been discussed in detail elsewhere.

SUMMARY

The structure of the truncated icosahedral fullerene C_{60}, which consists exclusively of pentagons and hexagons, can be generated from the regular (pentagonal) dodecahedron by omnicapping followed by dualization, namely the so-called leapfrog transformation. Analogous leapfrog transformations starting with the genus 3 Klein and Dyck tessellations consisting of 24 heptagons and 12 octagons, respectively, can generate possible highly symmetrical structures for allotropes of carbon and the isosteric boron nitride, $(BN)_x$. The Klein tessellation, alternatively described as a platonic {3,7} tessellation, corresponds to the Riemann surface for the multi-valued function $w = \sqrt[7]{z(z-1)^2}$ which can also described by the homogeneous quartic polyno-

mial $\xi^3\eta + \eta^3\omega + \omega^3\xi = 0$. The symmetry of this polynomial is related to the heptakisoctahedral automorphism group of the Klein tessellation of order 168. The Dyck or {3,8} tessellation can also be described by a Riemann surface which corresponds to the homogeneous Fermat quartic polynomial $\xi^4 + \eta^4 + \omega^4 = 0$. The symmetry of the Fermat quartic relates to the automorphism group of the Dyck tessellation of order 96.

REFERENCES

1. H. W. Kroto, A. W. Allaf, and S. P. Balm, *Chem. Rev.* **91** (1991) 1212–1235.
2. R. B. King, *J. Chem. Inf. Comput. Sci.* **38** (1998) 180–188.
3. S. Andersson, S. T. Hyde, K. Larsson, and S. Lidin, *Chem. Rev.* **88** (1988) 221–242.
4. A. L. Mackay and H. Terrones, *Nature* **352** (1991) 762.
5. D. Vanderbilt and J. Tersoff, *Phys. Rev. Lett.* **68** (1992) 511–513.
6. R. B. King, *J. Phys. Chem.* **100** (1996) 15096–15104.
7. (a) F. Klein, *Math. Ann.* **14** (1879) 428–471; (b) F. Klein, *Gesammelte Mathematische Abhandlungen*, Springer Verlag, Berlin, 1923, Vol. 3, pp. 90–136.
8. P. W. Fowler, *Chem. Phys. Lett.* **131** (1986) 444–450.
9. P. W. Fowler, J. E. Cremona, and J. I. Steer, *Theor. Chim. Acta* **73** (1988) 1–26.
10. R. L. Johnston, *J. Chem. Soc., Faraday Trans.* **87** (1991) 3353–3358.
11. P. W. Fowler and D. B. Redmond, *Theor. Chim. Acta* **83** (1992) 367–375.
12. P. W. Fowler and T. Pisanski, *J. Chem. Soc., Faraday Trans.* **90** (1994) 2865–2871.
13. A. Ceulemans, R. B. King, S. A. Bovin, K. Rogers, and P. W. Fowler, *J. Math. Chem.* **26** (1999) 101–123.
14. R. B. King, *Croat. Chim. Acta* **73** (2000) 993–1015.
15. W. Dyck, *Math. Ann.* **17** (1880) 510–516.
16. S. Hyde, *Acta Chem. Scand.* **45** (1991) 860–863.
17. H. E. Rauch and A. Lebowitz, *Elliptic Functions, Theta Functions, and Riemann Surfaces*, Williams and Wilkins, Baltimore, 1973.
18. F. Klein, *Vorlesungen über das Ikosaeder*, Teubner, Leipzig, 1884, or *Lectures on the Icosahedron*, Dover, New York, 1956, Part I, Chapter 2.
19. L. E. Dickson, *Modern Algebraic Theories*, Sanborn, Chicago, 1930, Chapter 13.
20. H. McKean and V. Moll, *Elliptic Curves*, Cambridge University Press, Cambridge, UK, 1997.
21. H. Levy, *Projective and Related Geometries*, MacMillan, New York, 1964, pp. 73–79.
22. B. Grünbaum and G. C. Shephard, *Tilings and Patterns: An Introduction*, Freeman, New York, 1989.
23. H. S. M. Coxeter and W. O. Moser, *Generators and Relations for Discrete Groups*, Springer-Verlag, Berlin, 1972.
24. H. S. M. Coxeter, *Introduction to Geometry*, Wiley, New York, 1961.
25. J.-F. Sadoc and J. Charvolin, *Acta Crystallogr., Sect. A* **45** (1989) 10–20.
26. H. Karcher and M. Weber, in: S. Levy (Ed.), *The Eightfold Way: The Beauty of Klein's Quartic Curve*, Cambridge University Press, Cambridge, UK, 1998, pp. 9–49.

SAŽETAK

Riemannove površine kao deskriptori za simetrične negativno zakrivljene strukture ugljikovih i borovih nitrida

R. Bruce King

Transformacije 'žabljeg' skoka počinju s Kleinovim i Dyckovim mozaicima 3. vrste koji se sastoje od 24 sedmerokuta i 12 osmerokuta. Svaki zasebno može generirati moguće visoko simetrične strukture za alotrope ugljika i izosteričnog borova nitrida, $(BN)_x$. Kleinov mozaik ploče, alternativno opisan kao platonski {3,7} mozaik, odgovara Riemannovoj površini za višeznačnu funkciju $w = \sqrt[7]{z(z-1)^2}$, koja se također može opisati homogenim polinomom $\xi^3\eta + \eta^3\omega + \omega^3\xi = 0$. Simetrija tog polinoma povezana je s heptakisoktaedarskom automorfnom grupom Kleinova mozaika reda 168. Slično tomu, Dyckov ili {3,8} mozaik može se opisati Riemannovom površinom koja odgovara homogenom Fermatovu polinomu $\xi^4 + \eta^4 + \omega^4 = 0$. Simetrija Fermatova polinoma povezana je s automorfnom grupom Dyckova mozaika reda 96.